

# Modeling the SAR Signature of Nonlinear Internal Waves

Ellen E. Lettvin

Applied Physics Laboratory, University of Washington

1013 NE 40<sup>th</sup> St, Seattle WA 98105

phone: (206) 685-1505 fax: (206) 543-6785

email: [ellenl@apl.washington.edu](mailto:ellenl@apl.washington.edu)

Grant Number: N00014-05-1-0368

## LONG-TERM GOALS

The long-term goal of this project is to develop a forward model that predicts the Synthetic Aperture Radar (SAR) signature of Non-Linear Internal Waves (NLIWs) under a range of environmental conditions.

## OBJECTIVES

The objectives of this project are to understand, quantify and model the factors that influence the SAR signature of internal waves (IWs) using *in situ* and remote measurements. To accomplish this we have been studying the variables that impact the both the surface roughness and the corresponding radar backscattering cross section.

Previous efforts focused on modeling the the modulation of surface waves by IWs using the action balance equation with source terms of energy input from the wind and energy loss from viscous dissipation. Our work seeks to include additional action source terms such as wave-wave interaction, generation of parasitic capillary waves and breaking waves.

## APPROACH

Two different methods have been pursued for this project. The first is based on the work of Lyzenga and Bennett (1988), who used the action balance equation (Equation 1) to model the spatial and temporal changes to the wave action spectral density arising from interactions with currents.

$$(1) \quad \frac{\partial N(k)}{\partial t} + (c_{gi} + u_i) \frac{\partial N(k)}{\partial x_i} - k_j \frac{\partial u_j}{\partial x_i} \frac{\partial N(k)}{\partial k_i} = Q(k) / \omega$$

The L&B model assumes sources and sinks (Q(k)) of action are input from the wind and energy loss from viscous dissipation. Using the action balance equation they predict the surface roughness modulation produced by the passage of an IW and the corresponding changes to backscattering cross section. We first implemented the L&B technique using the spectral model described in that paper; we subsequently modified the technique to use the Donelan and Pierson (1987) spectral model, which uses the same action source terms as the L&B model, but has more physically realistic directional characteristics.

We implemented a second technique (Kudryavtsev et al. (2003, 2005)) to predict the modulation of surface waves by IW-produced currents. This approach includes an innovative spectral model (Kudryavtsev, 1999) and additional action source terms associated with wave-wave interactions and

the generation of parasitic capillary waves. The action source terms of Kudryavtsev (2003) are given in Equation 2.

$$(2) \quad Q(k) = \omega^3 k^{-5} \left[ \beta_v(k) B(k) - B(k) \left( \frac{B(k)}{\alpha} \right)^n + I_{pc}(k) \right]$$

The first term on the right side,  $\beta_v(k) = \beta(k) - 4\nu k^2/\omega$  is ‘effective growth rate’, defined as wind growth rate less viscous dissipation, where  $\beta$  is given by

$$(3) \quad \beta(k) = C_\beta (u^*/c)^2 \cos^2 \varphi$$

$\varphi$  is the angle between wind and wave direction,  $k$  is wavenumber,  $\omega$  is radian frequency and  $C_\beta$  is given by Stewart (1974). The second term of (2), expresses nonlinear wave-wave interaction,  $\alpha$  and  $n$  are functions of  $k/k_\gamma$ , where  $k_\gamma = (g/\gamma)^{1/2}$ , which is the wavenumber of minimum phase velocity, and  $k_g = k_\gamma^2/k$ .

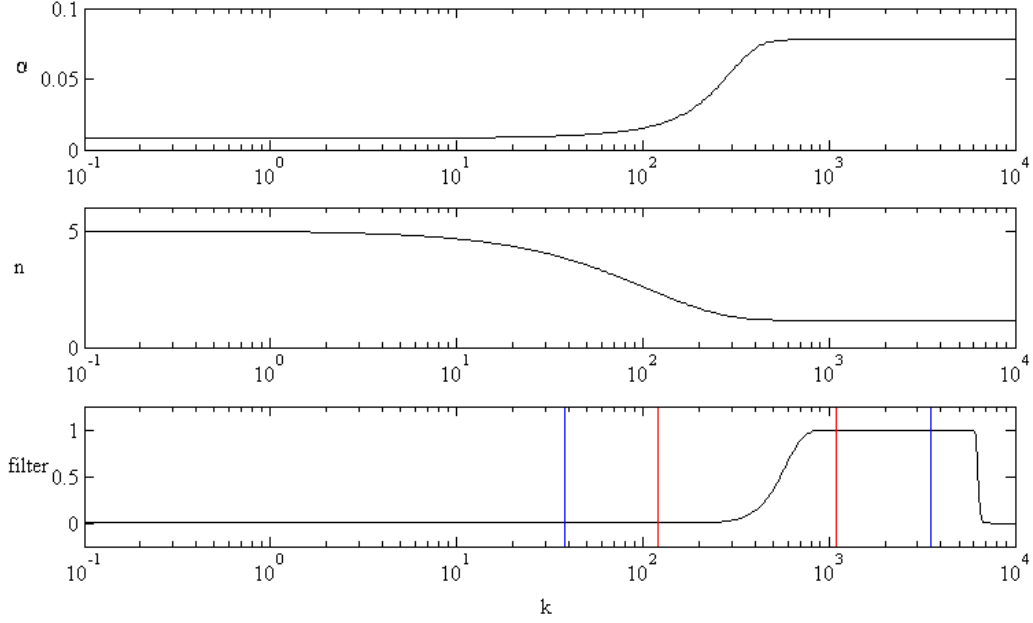
The third term in expression (2),  $I_{pc}$  captures the contribution of parasitic capillary waves. It is given by

$$(4) \quad I_{pc}(k) = \beta_v(k_g) B(k_g) \phi(k/k_g),$$

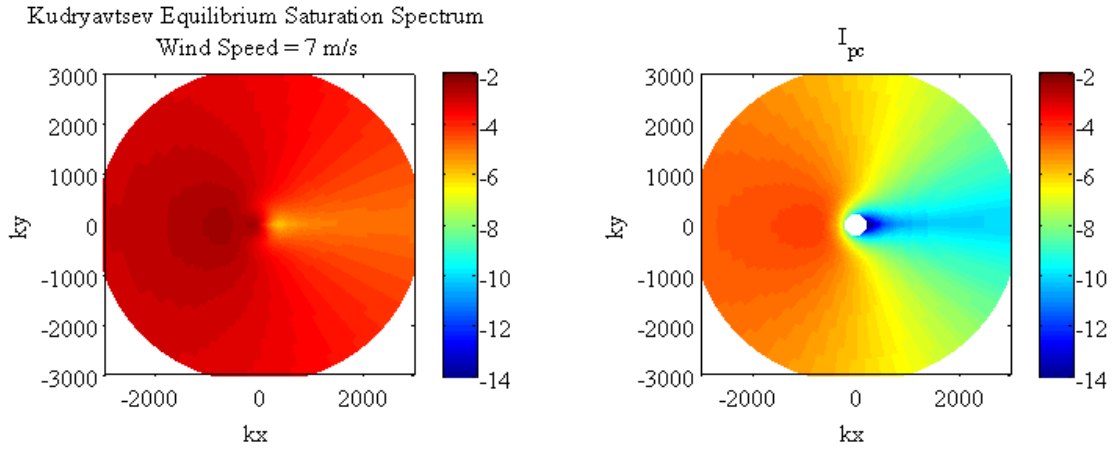
where  $\phi(k/k_g)$  is a filter function that restricts the action in  $k$ -space of the source term  $I_{pc}(k)$  to those gravity waves that generate parasitic capillary waves. The upper two panels of Figure 1 illustrate the wavenumber dependence of the terms  $\alpha$  and  $n$  in the action source term corresponding to wave-wave interaction. The bottom panel illustrates the wavenumber dependence the filter function for parasitic capillary waves. It is illustrated in the bottom panel of Figure 1.

Figure 2 illustrates how the magnitude of the  $I_{pc}$  source term varies relative to the magnitude of the Kudryavtsev spectrum. The panel on the left shows the two dimensional wavenumber spectral model of Kudryavtsev et al. (1999) for a wind of 7ms<sup>-1</sup>, in the  $\pi$  direction (wind blowing from right to left); the panel on the right illustrates the magnitude of the source term for parasitic capillary waves,  $I_{pc}$ , as a function of wavenumber and direction under the same conditions.

For both techniques, model inputs include: wind speed and direction, IW speed and direction, maximum surface current, current distribution and extent. Outputs for both include the 2-D wavenumber spectrum (expressed in terms of either action or saturation) as a function of position along a current profile. A comparison between the Donelan and Pierson (1987) and Kudryavtsev (1999) equilibrium spectral models is shown in Figure 3. The 2-D wavenumber spectra are the inputs to a scattering model that obtains predictions of backscatter for the modulated spectra.



**Figure 1.** Illustration of the wavenumber dependence of the exponent  $\alpha$  (upper panel), and denominator  $n$  (middle panel), in the Kudryavtsev (2003) model's action source term for wave-wave interactions. The bottom panel shows the filter function that is nonzero when conditions are favorable to generate parasitic capillary waves. The red and blue lines are included to show the relationship between gravity waves and the corresponding parasitic capillary waves.



**Figure 2.** Image on the left shows the Kudryavtsev (2003) equilibrium spectral model (saturation form in equilibrium); image on the right shows the corresponding action term associated with parasitic capillary waves,  $I_{pc}$  for a  $7\text{ms}^{-1}$  wind in the  $\pi$  direction. The color bar shows relative power levels in dB.

Backscatter predictions corresponding to the spectra described above, that have been modulated by interaction with the currents produced by an IW, are obtained using the stochastic, multiscale model of Plant (2004).

We are validating this technique in two ways: First, we are comparing model predictions with the 2-D wavenumber spectrum with *in situ* measurements of the 2-D wavenumber spectrum, such as those obtained by the ASIS buoy of Graber et al. In addition we are comparing model-derived backscatter predictions with backscatter measurements obtained both from ship-based radar and satellite-based SAR systems. Pursuant to obtaining the above-mentioned comparisons, we have assembled a database of collocated satellite and *in situ* observations from the field campaigns conducted as part of the NLIWI program in the South China Sea in 2005 and off the coast of New Jersey in 2006. These databases have been described in earlier reports.

## WORK COMPLETED

We have completed implementation of the Lyzenga and Bennett (1988) action modulation framework, using both the Lyzenga and Bennett spectral model and the Donelan and Pierson (1987) spectral model. These two spectral models are juxtaposed in Figure 3 to facilitate a comparison between these two techniques. The action modulation framework of Kudryavtsev et al. (2003) has also been successfully implemented and tested for several different wind speeds and directions, different surface current speeds and directions, and different surface current profiles, including a quasi-sinusoidal (based on an extrapolation obtained by D. Lyzenga based on measurements obtained by J. Moum during the 2006 New Jersey experiment) and a  $\text{sech}^2$  current distribution. Some illustrative examples of these will be shown in the next section.

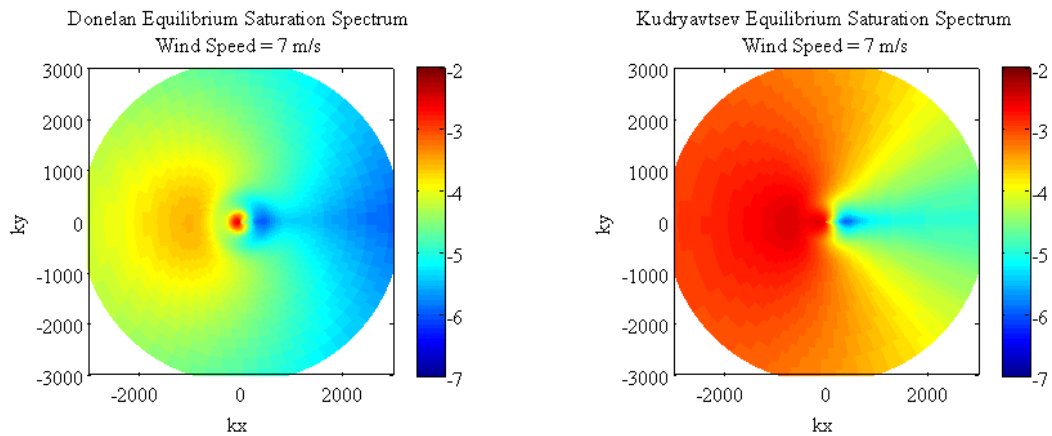


**Figure 3. 2-Dimensional wavenumber spectral model of Donelan et al. (1985), left panel, and Kudryavtsev et al. (1999), right panel, for wind speed  $7\text{ms}^{-1}$ ; wind direction =  $\pi$ . Color bar shows relative power in dB. Note color bar is different in Figures 2 and 3.**

All action modulation and surface wave spectral models have been implemented in a flexible, extensible web-based, password protected framework that can be accessed community-wide. Interested researchers will be given login and password information upon request.

## RESULTS

Implementation of both techniques has made it possible to identify and study the impact of trapped waves. Trapping is defined by either the time ( $>10,000$  cycles) or distance (1500 m) required to restore the action spectral density to its equilibrium state. Whether or not a particular wave will be trapped depends on conditions such as wavenumber, IW speed and direction, wind speed and direction, current maximum and current profile. Figure 4 shows a contour plot in the  $(x, k_x)$  plane ( $k_x > 0$ ) of the Hamiltonian of the action, computed along a characteristic curve, and illustrates a useful tool for identifying trapped waves. In this figure, those surface waves that originate within closed paths are trapped and surface waves that originate on an open path are not trapped.

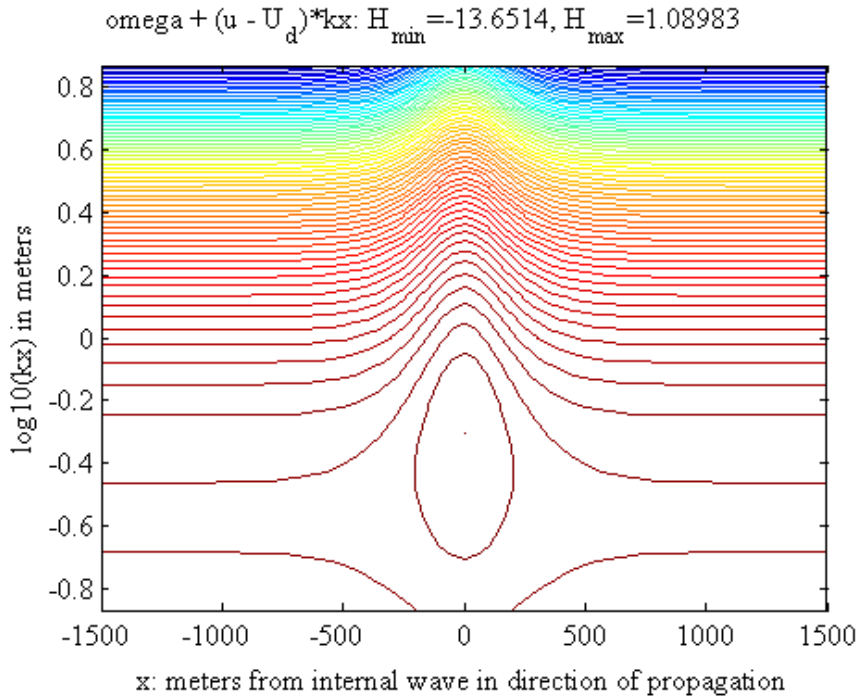


**Figure 4.** Here, we show the Hamiltonian of the action computed along a characteristic curve for a  $\text{sech}^2$  current profile that is defined varies over 3 km; the center of the  $x$  axis corresponds to the location of the current maximum, which is  $0.75\text{ms}^{-1}$ . The speed of the IW in this example is  $3\text{ms}^{-1}$ ; wind speed is  $5\text{ms}^{-1}$ , wind direction is  $\pi$ . NB: here  $k_y=0$ ,  $k_x>0$ , and the spectral model used is Donelan and Pierson (1987).

Figure 5 illustrates a technique that makes it possible to quantify the impact of the surface currents produced by an IW (specified by maximum current, velocity, current distribution, for a variety of current profiles, etc.), on a surface wave saturation spectrum. The upper panel illustrates the saturation spectrum as a function of  $x$ , location along the current profile. The lower panel illustrates the current magnitude as a function of  $x$ . Both panels are part of a movie that shows action modulation as a function of current, or position along  $x$ . The example shown in Figure 5 was derived by D. Lyzenga from current profile measurements obtained by J. Moum during the experiment conducted off NJ in 2006. The upper panel of the figure shows the first frame of a movie, corresponding to the equilibrium spectrum.

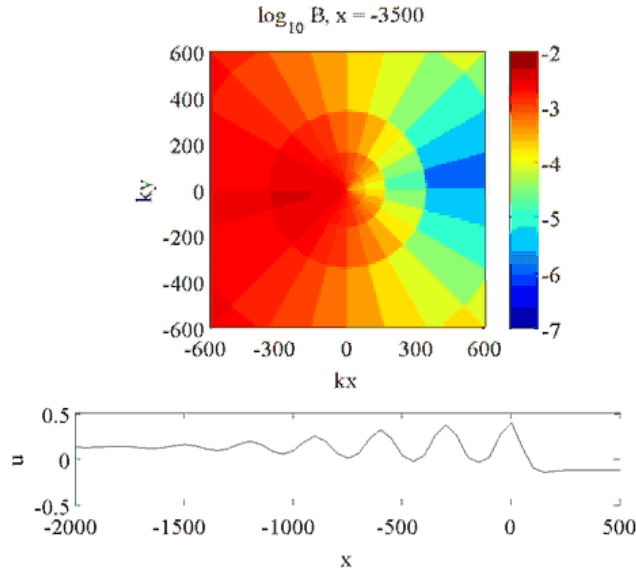


**Figure 5.**

Though we observe modulation of the saturation spectrum that arises from surface wave-IW interactions, the magnitude of modulation predicted by this model at the scale of Bragg wavenumbers for X-, C-, Ka- or Ku-band radars is too small. Efforts are underway to implement the Kudryavtsev et al. (2005) action modulation framework that includes a source term associated with the small-scale roughness generated by breaking waves.

### **IMPACT/APPLICATIONS**

The forward model being developed in this effort will be a key component of a capability for predicting and identifying IWs in satellite-based SAR imagery.

### **RELATED PROJECTS**

I am closely collaborating on this project with Dr. Bill Plant of APL-UW, Dr. David Lyzenga from the University of Michigan and Dr. Chris Wackerman from General Dynamics. I am also collaborating with Drs. Frank Henyey and Ren-Chieh Lien from APL-UW, who have consulted with me on project-related issues and have shared data with me obtained from the OR3, respectively.

### **PUBLICATIONS**

Lettvin E., 2007, Forward modeling of nonlinear internal waves, manuscript in preparation

Lettvin E., 2006, SAR Observations and Models of Nonlinear Internal Waves in the South China Sea, AGU 06 Conference Proceedings